Progress Towards Internal Transport Barriers at High Plasma Density Sustained by Pure Electron Heating and Current Drive in the FTU Tokamak

V. Pericoli Ridolfini[1], E. Barbato[1], P. Buratti[1], C. Castaldo[1], R. Cesario[1], V. Cocilovo[1], B. Esposito[1], E. Giovannozzi[1], G. Giruzzi[2], C. Gormezano[1], G. Granucci[3], M. Leigheb[1], M. Marinucci[1], F. Mirizzi[1], S. Nowak[3], L. Panaccione[1], S. Podda[1], Y. Peysson[2], M. Romanelli[1], A.N. Saveliev[4], P. Smeulders[1], C. Sozzi[3], O. Tudisco[1], FTU[1] & ECRH[3] teams

[1]*Associazione EURATOM-ENEA sulla Fusione, CR Frascati, Roma, Italy*
[2]*Association Euratom-CEA sur la Fusion DRFC/SCCP, CEA/Cadarache France*
[3]*Associazione EURATOM-ENEA sulla Fusione, IFP-CNR, Milano, Italy*
[4]*A.F. Ioffe Physico-Technical Inst. RAS, St. Petersburg, Russia*

e-mail contact of the main author: pericoli@frascati.enea.it

Abstract - Strong electron Internal Transport Barriers (ITBs) are obtained in FTU by the combined injection of Lower Hybrid (LH, up to 1.9 MW) and Electron Cyclotron (EC up to 0.8 MW) radio frequency waves. ITBs occur during either the current plateau or the ramp up phase, and both in full and partial current drive (CD) regimes, up to peak densities $n_{e0}>1.2\cdot10^{20}$ m^{-3}, relevant to ITER operation. Central electron temperatures $T_{e0}>11$ keV, at $n_{e0}\approx 0.8\cdot10^{20}$ m^{-3} are sustained longer than 6 confinement times. The ITB extends over a region where a slightly reversed magnetic shear is established by off-axis LHCD and can be as wide as r/a=0.5. The EC power, instead, is used either to benefit from this improved confinement by heating inside the ITB, or to enhance the peripheral LH power deposition and CD with off axis resonance. Collisional ion heating is also observed, but thermal equilibrium with the electrons cannot be attained since the e-i equipartition time is always 4-5 times longer than the energy confinement time. The transport analysis performed with both ASTRA and JETTO codes shows a very good relation between the foot of the barrier and the weak/reversed shear region, which in turn depends on the LH deposition profile. The Bohm-gyroBohm model accounts for the electron transport until $T_{e0}<6$ keV, but is pessimistic at higher temperatures, where often also a reduction in the ion thermal conductivity is observed, provided any magneto hydrodynamic activity is suppressed.

1. Introduction

The advanced scenario in the ITER tokamak foresees to establish a steady internal transport barrier (ITB) in order to achieve a high confinement. However, most present ITB experiments do not match the ITER features of high plasma density (line averaged value $\bar{n}_e\approx10^{20}$ m^{-3}) and dominant electron heating (α particle), with no central refueling or momentum input. On other tokamaks the ion ITBs are normally produced with ion heating techniques even at high density, and in case of neutral beam injection also refueling and momentum is provided. Electron ITBs instead, are produced at densities almost an order of magnitude smaller than in ITER. On the contrary, the availability of pure electron heating and current drive (CD) at reactor relevant plasma densities in the FTU tokamak has promoted the study of the onset, maintenance and properties of electron ITBs, as one of the leading programs.

In FTU we obtain robust ITBs by the combined injection of two radio frequency (RF) power sources: the lower hybrid (LH, f=8 GHz) and electron cyclotron (EC, f=140 GHz) waves, capable to deliver to the plasma up to 2 MW and 0.8 MW respectively. The LH waves have two main tasks: to control the current profile j(r) in order to built an ITB, by driving off-axis a large part of the plasma current (I_p), or even the whole, and also to heat the electrons. The EC waves instead, are used as a localized electron heating source with two main purposes: to benefit from the improved confinement by heating inside the ITB, with the EC resonance set on the magnetic axis, or to enhance the peripheral LH power deposition and current drive by heating the plasma off axis, with the resonance about 4 cm more external than the axis.

The paper is organized as follows. In Sec. 2 the experimental findings are described and the main characteristics of the ITBs in the operational space of FTU are presented. In Sec 3 the analysis of the transport properties and the interpretation of the experiment are given according to ASTRA and JETTO transport codes. In Sec. 4 the conclusions are drawn.

2. Experiment

Two main scenarios for the formation and maintenance of an ITB have been developed and studied up to now in FTU. In the first scenario, the RF waves are launched during I_p plateau, while in the second one the additional power is injected early during I_p ramp-up phase ($dI_p/dt \approx 2$ MA/s, typically). In FTU a low or even negative magnetic shear s is essential for the ITB onset, as for most tokamaks [1]. The shear s is defined as $s(r)= r/q \cdot dq/dr$, where r is the minor radius and q is the plasma safety factor, $q \approx aB_T/R_0B_\theta$ (R_0 is the major radius, a the plasma dimension, B_T and B_θ the toroidal and poloidal magnetic fields). A reversed shear can be steadily sustained in FTU only by off-axis LH current drive (LHCD), because there are no other effective current sources: no neutral beam injection and negligible bootstrap current (usually $I_{boot}/I_p \approx \leq 5\%$). Production of ITBs requires not only that the CD current fraction I_{LH}/I_p be larger than 50% at least, but also that the MHD (magneto hydro-dynamic) activity be negligible to avoid a fast current diffusion. The second scenario (early LHCD) is studied to possibly exploit pre-existing flat or reversed shear due to non-relaxed ohmic j(r) profiles, in view of improving the ITBs performance and of extending their plasma parameter space.

In the first scenario the EC power is launched with the resonance located very close to the magnetic axis in an almost MHD quiescent plasma, after the LHCD has built the barrier. The best results are obtained under full CD conditions, because in this case the j(r) profile tends to be steady even for large variation of the central electron temperature caused by central EC heating (ECH), ΔT_{e0}>4 keV. This has been inferred in a previous work [2] from the stability of the radial profile of the fast electron bremsstrahlung, emitted by the LH generated e^- suprathermal tail, and it is confirmed by code simulations. The reason is twofold: the electrical resistivity profile, associated to $T_e(r)$ change, does not affect noticeably j(r) because the toroidal electric field is quite negligible, and the LH absorption undergoes a sort of positive feedback. Indeed, the ITB foot occurs in the vicinity of the maximum LH absorption radius, where the shear s becomes low or reversed. If the ITB is heightened, the steeper ∇T_0 further favors the local LH power deposition. This is only an outline of the main features of an ITB formation in FTU: minor changes in j(r) do still occur as indicated by small sized MHD activity observed inside the ITB during the ECH phase (see below).

We assume that an ITB is formed when the maximum value of the quantity $\rho^*_T=\rho_{L,s}/L_T$ along the radius becomes larger than the threshold value of 0.014, which is appropriate for JET [3]. $\rho_{L,s}$ is the Larmor radius of the ions moving at the sound velocity, and $L_T=T_e/(dT_e/dr)$ is the local characteristic length of the electron temperature T_e. Fig. 1 shows the main characteristics of a quasi-steady ITB at moderately high density in full LHCD conditions. From top to bottom are shown the time traces of: a) the line averaged and central density ($\bar{n}_e$, n_{e0}); b) the central electron temperature T_{e0}; c) the height or the strength of the barrier, estimated from $\rho^*_{T,Max}$, the maximum of ρ^*_T; d) the radial extension of the ITB, defined as the radius where ρ^*_T exceeds the threshold; e) the applied RF power (P_{LH} and P_{ECH}). Fig. 1 clearly shows that the barrier is virtually steady: its width stays constant for as long as LHCD is applied and it is not affected by the ECH power, as expected if no variation in j(r) occurs.

Figure 2 presents the typical time evolution for the second scenario. From top to bottom we plot: a) central and line averaged density, b) central electron temperature, c) ITB radial extension, d) fusion neutron yield; e) applied RF power. The magnetic field is adjusted to have the EC resonance some cm off axis (R_{res}=1 m, R_0=0.935 m) in order to increase and broaden $T_e(r)$. This should assist the peripheral deposition of the LH power, which otherwise would be absorbed more centrally in the low density plasma existing at that time. Very high temperatures (T_{e0}>11 keV) are thus achieved and strong barriers are established, with ρ^*_T>0.05 and no MHD activity. The ITB footprint expands from r/a ≈1/3 to r/a>0.5 in the time window 0.1-0. 3 s, following the outward shift of the LH deposition. This in turn is caused primarily by the decrease of q(a) with

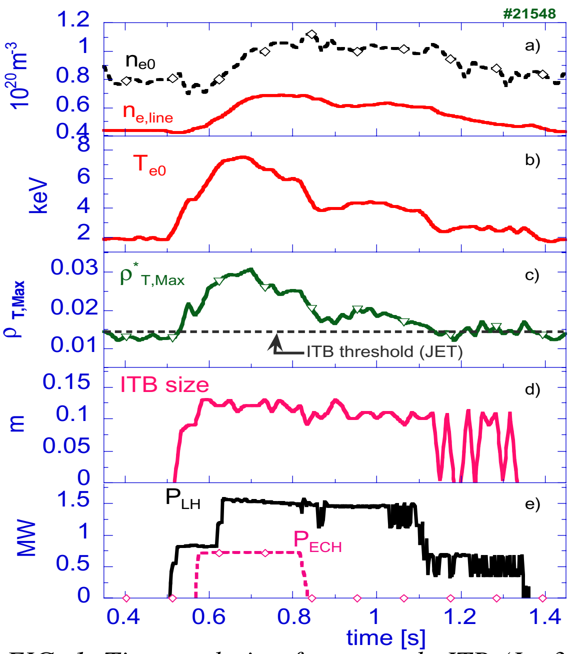

FIG. 1. *Time evolution for a steady ITB (I_p=360 kA, B_T=5.3 T, EC resonance on axis) of: a) peak and line averaged density; b) peak electron temperature; c) normalized ion Larmor radius (max along the radius) $\rho^*_{T,Max}$; d) ITB radial size; e) applied RF power*

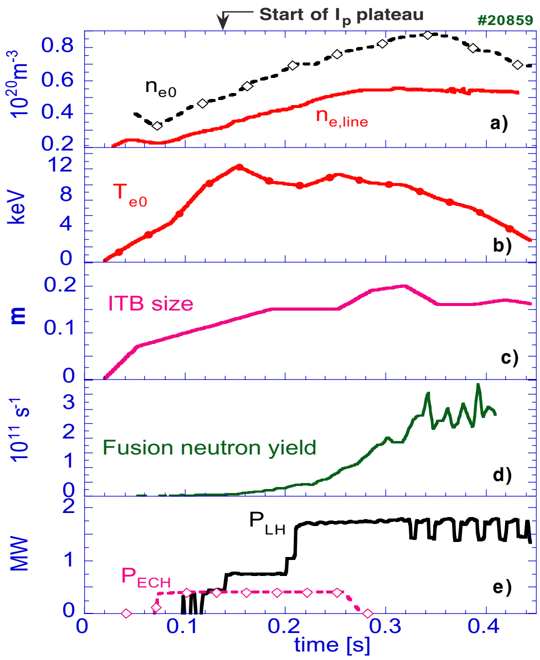

FIG. 2. *Time evolution for an ITB built during current ramp-up (I_p=500 kA, B_T=5.5 T EC resonance 4 cm off-axis). a) peak and line density; b) central electron temperature; c) radial ITB size; d) neutron yield; 5) applied RF power. T_{e0}≈11 keV until n_{e0}≈0.8·10^{20} m^{-3}*

some contribution also from the increase of the density (see discussion in Sec. 3). The ITB end coincides with an MHD instability starting at 0.34 s, which after some tens of ms slows down and finally locks at 0.43 s causing the plasma disruption. In the MHD quiescent phase however, some impurity accumulation occurs, differently from the first scenario (Fig. 1) which is never totally MHD free. The cause for the peaking of the Z_{eff} profile (average ion charge) is an increase of the impurity inward pinch velocity respect to non-ITB discharges, according to transport codes, based on the high resolution far UV spectroscopy of highly ionized states of Fe and Mo [4] (Mo is the FTU main impurity). The radial diffusion instead remains substantially unchanged.

The onset of the MHD activity is the main reason why a true stationarity has not yet been reached for this second scenario. While the effect of prolonging the ECH pulse is still to be investigated, clearly a longer steady phase could be achieved in almost full CD conditions. With the LH and EC power now available, this would imply to decrease I_p from 0.5 to 0.35 MA, but the shorter ramping up phase would require to anticipate the LH pulse at a time when the plasma position is still not enough controlled for a satisfactory LH coupling. Even if this scenario is not strictly steady, its study is important for application to the advanced tokamak scenarios requiring high plasma current, as pointed out in [5]. Moreover we got the FTU highest central electron pressure, p_{e0}>0.15 MPa (≈1.6 bar), and very high temperatures (T_{e0} even ≥15 keV), close to the FTU record [6] but lasting longer, about 5-6 energy confinement times. In these conditions the electron thermal diffusivity χ_e can be as small as 0.1-0.5 m^2/s within the barrier, with no degradation with respect to lower temperature ITBs, and the ion transport also appears reduced, as it will be shown in Sec. 3.

In FTU ITBs the ions, are heated collisionally by electrons, as shown by the large increase of the fusion neutron yield in Fig. 2 c). The central ion temperatures are in the range T_{i0}=1.2–1.6 keV, with an increment during the ITB ΔT_{i0}≈0.2–0.3 keV. Larger ΔT_{i0} are prevented by the fact that the e-i thermal equipartiton time τ_{eq} is much longer than the energy confinement time τ_E (for discharge of Fig. 2 τ_{eq}≈0.18 s τ_E≈0.02 s). To obtain ITBs with τ_{eq}≈τ_E

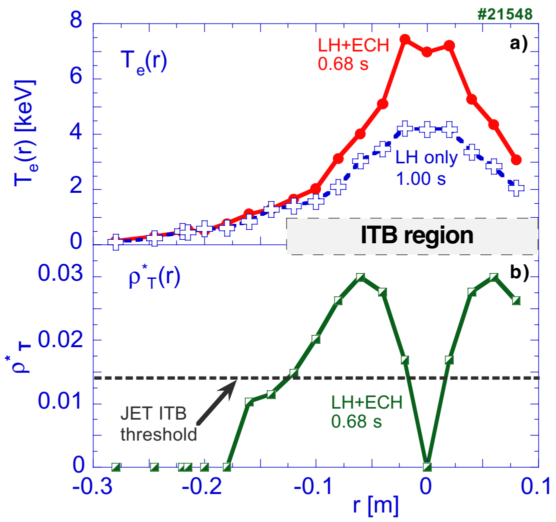

FIG. 3. Radial profiles for #21548 (same as in Fig. 1) of: a) electron temperature during the full power (LH+ECH) and the LH only phases; b) normalized ion Larmor radius, $\rho^*_{T,Max}$. Note how the ECH effect is bounded inside the ITB

we should raise either n_e or I_p, in order to either decrease τ_{eq} or increase τ_E, but this would demand a proportionally higher P_{LH}, which is presently not available in FTU, unfortunately.

The effect of central ECH is to reinforce the ITB as shown in Fig 3 where two $T_e(r)$ profiles with and without ECH are compared for the discharge shown in Fig.1. During the ECH phase the electron temperature increases only inside the barrier and very slightly outside, giving a direct experimental evidence of the good confinement properties of the ITB region. Indeed, the JETTO code simulation of this shot does not record any variation in t_E after the EC power switch-off, despite in the ECH phase the larger total power (2.25 against 1.45 MW) would imply a decrease of τ_E by 1.25 times approximately.

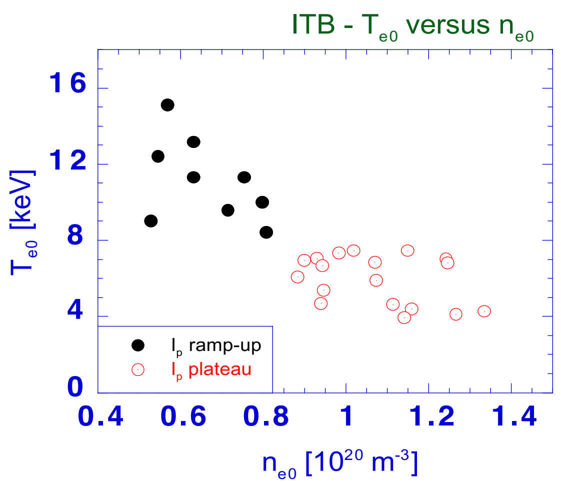

FIG. 4. Behavior of the ITB central electron temperature as the density is varied. ● refer to I_p ramp-up phase, O to plateau

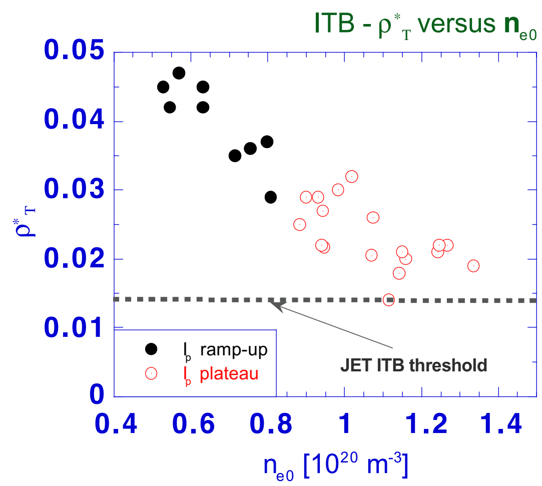

FIG. 5. Behavior of the ITB strength, namely $\rho^*_{T,Max}$ as the density is varied. ● symbols refer to the I_p ramp-up phase, O to the plateau

The behavior of the ITBs as the density is varied is shown in Figs. 4 and 5. T_{e0} and $\rho^*_{T,Max}$ are respectively plotted versus the central plasma density n_{e0}. The best ITBs occur when LH is applied in the I_p ramp-up phase, because we benefit from the not yet fully relaxed j(r) profile,but unfortunately in FTU it is not possible to raise substantially the density during this phase. As expected, T_{e0} decreases when n_{e0} increases, due to the simultaneous decrease of the available power per particle. The same behavior of $\rho^*_{T,Max}$ suggests that also the strength of the barrier suffers from the lack of power: as the power is reduced the barrier weakens until it survives no more. The $\rho^*_{T,Max}$ drop does not seem instead clearly related to the ratio I_{LH}/I_p, which measures the depth of the shear reversal.

3. Transport analysis

The most significant ITBs discharges have been independently analyzed with two transport codes: JETTO [7] and ASTRA [8]. JETTO is preferentially used as an interpretative tool, where the radial profile of T_e and n_e are assigned by the experiment and the transport properties are deduced by trying to match the time evolution of the most important plasma quantities, namely the loop voltage, the radiated power, the neutron yield and the visible bremsstrahlung radiation. A 1D Fokker-Planck Bonoli code and an EC ray tracing code [9] fix the radial deposition profiles of the LH, together with CD, and ECH power respectively. The involved uncertainties are below the of the experimental inaccuracies, as deduced in a previous work [10] from the good agreement between the radial profile of the hard X-ray (photon energy range: 60 – 80 keV) emitted by the LH generated fast e^- tail and the calculated profile $j_{LH}(r)$. Conversely, ASTRA is mostly used as a predictive code. The electron thermal diffusivity χ_e is modeled following the shear dependent Bohm-gyroBohm (BgB) model [11]:

$$\chi_e = D_B (a/L_T) \cdot (\alpha_B q^2 f(s) + \alpha_{gB} \rho^*) \quad (1)$$

Here the function f(s), $f(s)=s/(1+s^3)$ for $s \geq 0$ and $=0$ elsewhere, connects the T_e and q profile evolution, $D_B=cT_e/(16eB)$, is the Bohm diffusion coefficient and ρ^* is the ratio of the electron Larmor radius to the plasma minor radius a. The coefficients α_B and α_{gB} are normally between 1 and 3 times those given in Ref. [11] and for each shot are adjusted to match the experimental $T_e(r)$ before the main heating phase. A fast 1D ray tracing deposition code coupled to ASTRA [12] calculates at each time step the LH deposition, self-consistently with the current and heat diffusion equations and the structure of the electron distribution function is evaluated as a function of the radius. The poloidal extension of the FTU launcher (≈80°) is also taken into account. The code tries to match of the experimental $T_e(r)$ profile in its time evolution, in addition to the same other main plasma quantities as for JETTO. In both codes the ion transport is modeled imposing an anomaly factor to the neoclassical diffusivity.

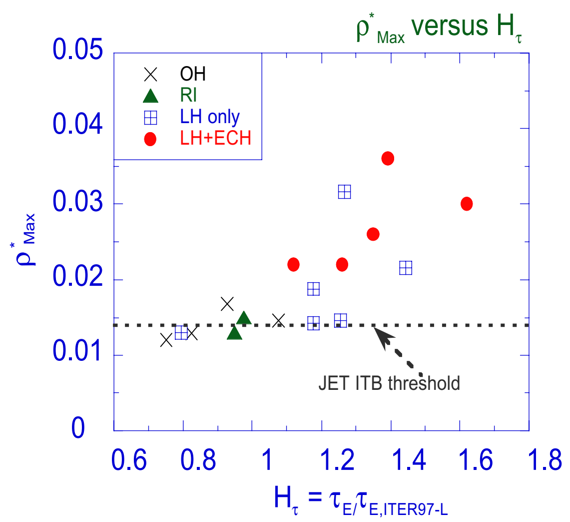

FIG. 6. Normalized ion Larmor radius $\rho^*_{T,Max}$ plotted versus H_τ ($=\tau_E/\tau_{E,ITER97-L}$ confinement enhancement factor). H_τ starts increasing very close to where $\rho^*_{T,Max}$ exceeds the JET threshold. 100% LH absorption is always assumed

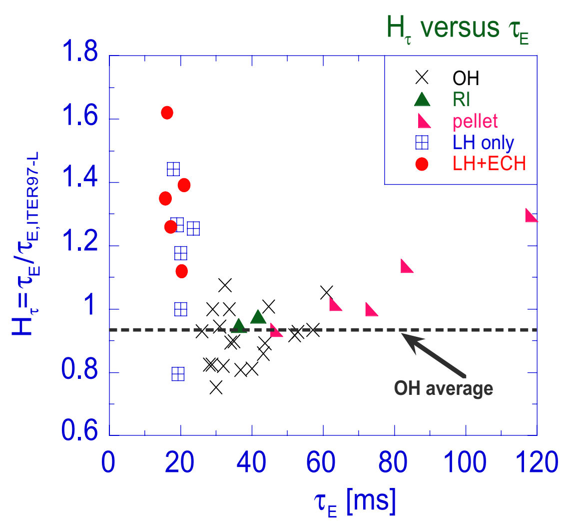

FIG. 7. Variation of the confinement enhancement factor H_τ ($=\tau_E/\tau_{E,ITER97-L}$) versus τ_E. In terms of H_τ, the LH+ECH ITBs show the same quality as the pellet discharges, even though at much lower density and current

The results of the transport analysis concerning the global properties of the ITB discharges are illustrated in Figs. 6 and 7. In Fig 7 $\rho^*_{T,Max}$ is plotted versus the confinement enhancement factor

($H_\tau=\tau_E/\tau_{E97}$, ratio of τ_E to the ITER97-L scaling). Different time windows during OH, LH only, and LH+ECH phases are considered.

The strongest ITB phases, obtained with the combined action of the LH and EC waves, show the highest confinement. Moreover, the depart from the L-scaling occurs very close to the ρ^*_T value of 0.014, assumed as the threshold for the onset of an ITB in JET [3]. The clear increase of H_τ factor with $\rho^*_{T,Max}$ demonstrates the effect of the strength of the barrier on the global properties of the plasma. In Fig. 7 we plot the factor H_τ versus τ_E for comparison of the ITB shots with a more extended FTU data set, including discharges concerning the RI (radiation improved) mode and the pellet injection [13]. The ITB plasmas have $H_\tau\approx1.3$-1.6, even higher than the pellet shots at the highest densities and currents, $n_{e0}>7\cdot10^{20}$ m^{-3}, $I_p=1.2$-1.6 MA. The absolute level of the energy confinement is however lower for the reasons that the good confinement regimes in FTU are at high currents ($I_p>1$ MA), where there is no possibility to modify j(r) to the extent required by an ITB, with the present LH power level. For the same reason also the very high density regimes ($n_{e0}>1.5\cdot10^{20}$ m^{-3}) are inaccessible to ITBs in FTU.

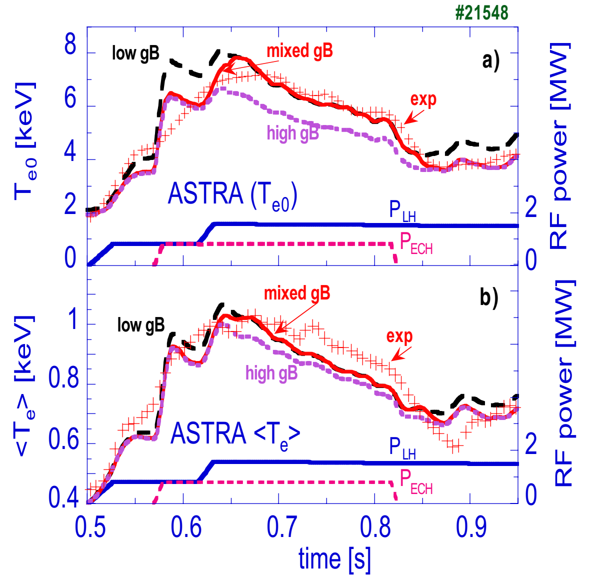

FIG. 8. Comparison between experiment (+) (#21548, also in Fig. 1) and the time traces of the central and volume temperature (a) and b) respect.) predicted by ASTRA. In the long dash case (low gB) the gyroBohm coefficient is 1.94 smaller than in the short dash case (high gB). The full line case switches from the higher to the lower gB coefficient during the full power/high T_{e0} phase. This is apparently the only way to fit experiment in the frame of the BgB model

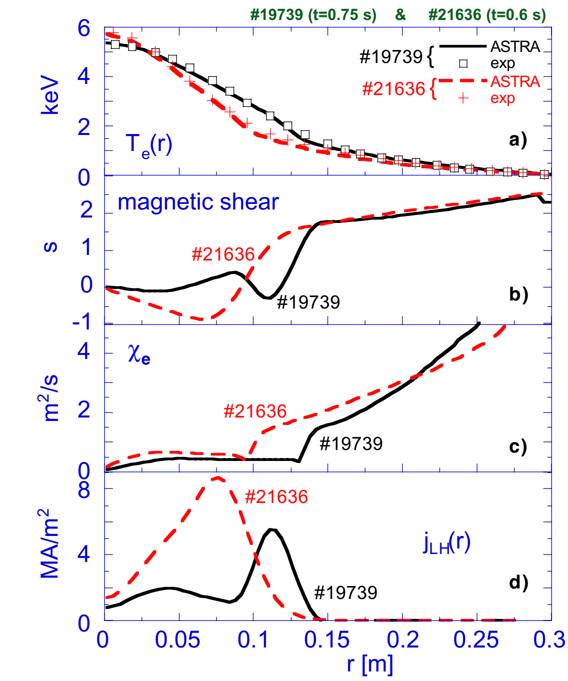

FIG. 9. Computed radial profiles (ASTRA) for #19739 (q(a)=5.6, 0.75 s, —–) and #21636 (q(a)=8, 0.6 s, - - -) of: a) temperature (exp. points are also shown); b) magnetic shear s; c) electron thermal conductivity χ_e; d) driven LH current. The discharge with higher q has all profiles shifted outwards

Figure 8 shows that the BgB model cannot reproduce the time evolution of either T_{e0} (frame a) or the volume temperature <T_e> (frame b) with single value for α_{gB} (see Eq. 1) if $T_{e0}>6$ keV. The electron thermal diffusivity in the full power phase must be set 1.94 times lower than in the low power case. This confirms what was found in the first experiences with an ITB [2] on FTU at much lower power and density. Conversely, if $T_{e0}\leq6$ keV, single value of α_{gB} is sufficient for the whole time evolution. We expect that some mechanism of turbulence stabilization is responsible for the reduction of α_{gB}, but the present available data do not allow any conclusive statement. One possible candidate is the stabilization associated to large pressure gradients (finite β effect) found by gyro-kinetic simulations in Ref [14] and invoked also in DIII-D experiments [15].

Concerning the χ_e radial profile apparently a rather localized barrier develops. A sharp drop, down to values $\chi_e=0.1$-0.5 m^2/s, occurs at the barrier footprint, which is located just where the magnetic shear becomes flat or slightly reversed (s≈0). The radius where this occurs is in turn determined by the LH absorption, and shifts outwards if the safety factor q is lowered. This is shown in Fig. 9 where we compare two discharges with different q (#19739 with q(a)=5.6 and #21636 with q(a)=8). The computed profiles of $T_e(r)$, s(r), $\chi_e(r)$ and $j_{LH}(r)$ are plotted in the frames from a) to d). It appears clearly that the lower q gives origin to ITB of larger size as a consequence of a more peripheral LH power deposition, in good agreement with the experiment. The same outward shift of the LH deposition is observed in the scenario with ramping I_p (see Fig. 2) during the expansion of the ITB, as a result more of the simultaneous decrease of q(a), than of the density increase.

Ions, which in FTU ITBs are not strongly collisionally coupled to electrons, behave almost neoclassically with an anomaly factor around 2. But it is significant that during the high power phase a reduction in χ_i may occur, as pointed out in describing Fig. 2. Simulations with JETTO can reproduce the fusion neutron yield of #20589 (Fig. 2, frame d) only if the ion anomaly is reduced to 1.1 from the previous value of 1.7, in the time window 0.24-0.33 s.

4. Conclusions

Stationary electron ITBs have been obtained in FTU at plasma density relevant to ITER operations, by applying simultaneously the LH and EC power up to levels of about 1.9 MW and 0.7 MW respectively. Central temperature T_{e0}>6 keV at central plasma densities $n_{e0}> 1.2\cdot10^{20}$ m^{-3} ($\bar{n}_e \geq 0.8\cdot10^{20}$ m^{-3}), and T_{e0}>15 keV at $n_{e0} \approx 0.8\cdot10^{20}$ m^{-3} ($\bar{n}_e \approx 0.5\cdot10^{20}$ m^{-3}) can be maintained longer than 6 energy confinement times. The global energy confinement time can exceed the ITER97-L thermal scaling up to a factor 1.6. FTU has therefore demonstrated that to operate close to ITER density and magnetic field does not prevent the formation of an ITB.
Off-axis LHCD is used to modify j(r) in order to produce q(r) with a negative/flat shear s: the ITB develops for $r \leq r_{s\leq0}$, and can extend over half the radius. ECH is used either to profit from the reduced transport by heating the plasma at the center, or to assist off-axis LHCD. Temperature profiles with $\rho^*_{T,Max}$>0.04 (the JET threshold value is ρ^*_T=0.014 [3]) or $R/L_T \approx 20$ at the foot of the barrier ($R/L_T \approx 7$ is typical of $T_e(r)$ stiffness [16]) are obtained. At the ITB footprint ($r= r_{s\leq0}$) the electron thermal diffusivity drops quickly to value 0.1-0.5 m^2/s. The shear dependent Bohm-gyroBohm model for χ_e accounts for the time evolution of $T_e(r)$, for T_{e0} up to 6 keV, whereas at higher T_{e0} the gyroBohm coefficient needs to be reduced, indicating a better confined energy. Ion heating via e-i collisions is observed, consistent with ion diffusivity 1-2 times the neoclassical value, but during the strongest ITBs ion transport must be reduced to fit the neutron fusion yield.

The LHCD physics is satisfactorily described by the ray-tracing codes, which can account for the fact that the ITB size increases when q(a) decreases, by showing that the LH deposition, and the shear inversion radius with it, shifts outwards. The same mechanism can explain also why the ITB expands in time when it is created during the I_p ramp-up phase.

ACKNOWLEDGEMENT

The authors acknowledge the professional and constant support of the technicians involved in the LH system, M. Aquilini, S. Di Giovenale, T. Fortunato, P. Petrolini, and in the ECH system V. Mellera, V. Muzzini.

References

[1] BARBATO E. et al, Plasma Phys. Control. Fusion, **43**, No 12A, (2001) A287
[2] PERICOLI RIDOLFINI, V., et al. “Synergy between LH and ECH Waves in the FTU Tokamak”, Radiofrequency Power in Plasmas, (14th Top. Conf. on RF Power in Plasmas, Oxnard, CA, USA 7-9 May 2001), p. 225, American Institute of Physics, New York (2001)
[3] TRESSET, G., et al, Nucl. Fusion, **42** (2002) 520
[4] CARRARO L. et al., "Impurity transport simulation in Radiatively Improved and ITB plasmas in FTU", 29th EPS Conf, on Controlled Fusion and Plasma Physics, June 16-21 2002, Montreux (CH) contribute n. P4.042

[5] CASTALDO, C. et al. Phys Plasmas **9** (2002) 3205
[6] ALLADIO, F. et al, “Overview of the FTU results”, Proc 18th IAEA Fusion Energy Conf., Sorrento, Italy, 4-10 Oct 2000, paper IAEA-CN-77/OV/2
[7] CENACCHI, G., TARONI, A., "The JET equilibrium-transport code for free boundary plasmas (JETTO)", Proc. 8th Computational Physics. Computing in Plasma Physics, Eibsee, BRD, 12-16 May 1986, Europ. Physical Society, Geneve **10D** (1986) 57
[8] PEREVERZEV, G.V., et al., Nucl. Fusion **32** (1992) 1023
[9] NOWAK, S., OREFICE, A., Phys. Plasmas **1**, (1994) 1242
[10] PERICOLI RIDOLFINI, V., et al., “Combined LH and ECH Experiments in the FTU Tokamak”, Proc 18th IAEA Fusion Energy Conf., Sorrento, Italy, 4-10 Oct 2000, IAEA-CN-77/PDP7
[11] VLAD, G. et al., Nucl. Fusion **38** (1998) 557
[12] ESTERKIN, A.R., and PILYA, A.D., Nucl. Fusion **36** (1996) 1501
[13] ANGELINI, B., et al., “Overview of the FTU results”, Proc 19th IAEA Fusion Energy Conf., Lyon, France, 14-19 October 2002, paper OV/4-5
[14] BEER, M.A., et al., Phys. Plasmas **4** (1997) 1792
[15] DOYLE, E.J., et al, “Progress toward increased understanding and control of internal transport barriers on DIII-D” Proc 18th IAEA Fusion Energy Conf., Sorrento, Italy, 4-10 Oct 2000, IAEA-CN-77/EX6/2.
[16] JACCHIA, A. et al, “Gradient Length Driven Transport in EC Heated FTU Tokamak” Radiofrequency Power in Plasmas, (14th Top. Conf. on RF Power in Plasmas, Oxnard, CA, USA 7-9 May 2001), p. 342, American Institute of Physics, New York (2001)